

# Synthesis, resolution, stereochemistry, and molecular modeling of (*R*)- and (*S*)-2-acetyl-1-(4'-chlorophenyl)-6,7-dimethoxy-1,2,3,4-tetrahydroisoquinoline AMPAR antagonists

Rosaria Gitto,<sup>a</sup> Rita Ficarra,<sup>a</sup> Rosanna Stancanelli,<sup>a</sup> Marta Guardo,<sup>a</sup> Laura De Luca,<sup>a</sup> Maria Letizia Barreca,<sup>a</sup> Benedetta Pagano,<sup>a</sup> Archimede Rotondo,<sup>b</sup> Giuseppe Bruno,<sup>b</sup> Emilio Russo,<sup>c</sup> Giovanbattista De Sarro<sup>c</sup> and Alba Chimirri<sup>a,\*</sup>

<sup>a</sup>*Dipartimento Farmaco-Chimico, Università di Messina, Viale Annunziata, I-98168 Messina, Italy*

<sup>b</sup>*Dipartimento di Chimica Inorganica, Chimica Analitica e Chimica Fisica, Università, Vill. S. Agata, I-I-98166 Messina, Italy*

<sup>c</sup>*Dipartimento di Medicina Sperimentale e Clinica, Università Magna Græcia, Via T. Campanella, I-88100 Catanzaro, Italy*

Received 22 January 2007; revised 24 May 2007; accepted 25 May 2007

Available online 31 May 2007

**Abstract**—Recently we identified (*R,S*)-2-acetyl-1-(4'-chlorophenyl)-6,7-dimethoxy-1,2,3,4-tetrahydroisoquinoline (**6**) as a potent non-competitive AMPA receptor antagonist able to prevent epileptic seizures. We report here the optimized synthesis of compound **6**, its resolution by chiral preparative HPLC, and the absolute configuration of (*R*)-enantiomer established by X-ray diffractometry. The biological tests of the single enantiomers revealed that higher anticonvulsant and antagonistic effects reside in (*R*)-enantiomer as also suggested by molecular modeling studies.

© 2007 Elsevier Ltd. All rights reserved.

## 1. Introduction

Glutamate (Glu), the major stimulatory neurotransmitter in the central nervous system (CNS) of vertebrates, interacts with ionotropic (iGluRs) and metabotropic (mGluRs) receptors.<sup>1</sup> The AMPA receptors (AMPA) are members of the iGluR family and play important roles for neurotransmission in the CNS and in synaptic plasticity that underlies learning processes and memory.<sup>2</sup> Over-stimulation of the AMPARs is, however, thought to be involved in neuronal cell death caused not only by hypoxic conditions such as stroke but also neurodegenerative disorders such as Huntington's disease, epilepsy, etc. Therefore, AMPAR antagonists have been recognized to be potential therapeutic agents for such disorders.<sup>3–5</sup> The unwanted side effects of competitive AMPAR antagonists steered the search for new agents that inhibit AMPARs in a non-competitive mode of action and different molecules were identified such as

GYKI 52466 (**1**), talampanel (**2**), CFM-2 (**3**), YM928 (**4**), and ZK187638 (**5**) (Chart 1).<sup>3</sup>

Using a molecular modeling approach, we have previously developed a 3-D pharmacophore model for non-competitive AMPAR antagonists.<sup>6</sup> Based on this study, the tetrahydroisoquinoline scaffold emerged as a template for the development of a new class of ligands that mapped well all chemical requirements suggested by the pharmacophore hypothesis. As validation of our model we synthesized various 1-aryl-6,7-dimethoxy-1,2,3,4-tetrahydroisoquinolines and found that some derivatives demonstrated marked anticonvulsant effects in various seizure models and noncompetitive AMPAR antagonism.<sup>7–9</sup> In particular, we found that the (*R,S*)-2-acetyl-1-(4'-chlorophenyl)-6,7-dimethoxy-1,2,3,4-tetrahydroisoquinoline (**6**, Chart 1) interacts with AMPA receptor complex in a selective and non-competitive fashion and consistently suppressed AMPA responses at a 100-fold lower dose than GYKI 52466 (**1**), the prototype of non-competitive AMPA receptor antagonists.<sup>7</sup> Compound **6** also demonstrated good uptake by the brain as well as metabolic stability<sup>10</sup> and was studied as a potential ligand for in vivo imaging of AMPA receptors using PET.<sup>11</sup>

**Keywords:** Tetrahydroisoquinoline; Microwave-assisted synthesis; Anticonvulsant; AMPA-antagonist; Molecular modeling; Enantiomeric resolution; X-ray crystal structure.

\*Corresponding author. Tel.: +39 0906766412; fax: +39 090355613; e-mail: [chimirri@pharma.unime.it](mailto:chimirri@pharma.unime.it)

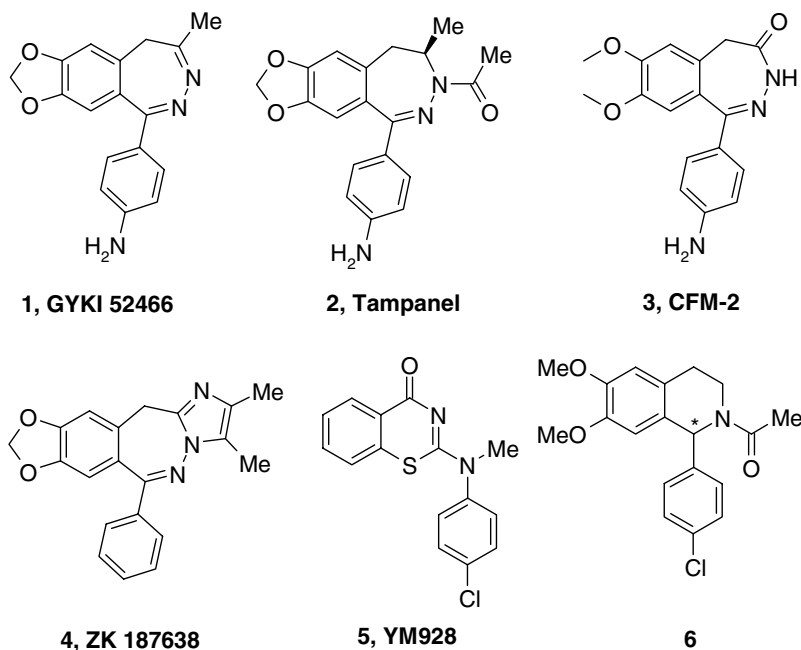


**Chart 1.** Non-competitive AMPA receptor antagonists.

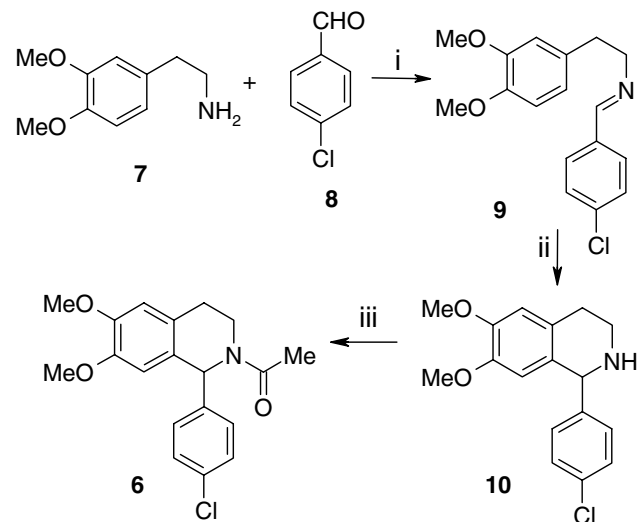
All these studies were carried out on compound **6** as racemic mixture but a different level of activity or specificity of action of the two enantiomers was to be expected. In fact, it is well known that the enantiomers of chiral drugs generally show significant differences in their pharmacokinetics, pharmacodynamics, and adverse reactions. As a consequence, there is an increasing demand for the production of enantiomerically pure compounds in fine chemistry and the pharmaceutical industry.

Therefore, with the aim of elucidating the enantiopharmacological profile of compound **6** we describe in this paper its chiral resolution by rapid and efficient high-performance liquid chromatography (HPLC) method, the *in vivo* and *in vitro* activity of the resolved enantiomers, and the determination of the absolute stereochemistry of the more active one, by X-ray analysis. Finally, the results obtained were employed in a molecular modeling study in order to explain the different level of activity of the two isomers and to confirm the structural requirements influencing the potency of this class of tetrahydroisoquinoline AMPAR antagonists. We also report here an optimized synthesis of (*R,S*)-2-acetyl-1-(4'-chlorophenyl)-6,7-dimethoxy-1,2,3,4-tetrahydroisoquinoline (**6**) through a new solvent-free microwave-assisted approach which requires reduced reaction times and is suited to large scale production.

## 2. Results and discussion

In a previous paper we reported the preparation of (*R,S*)-2-acetyl-1-(4'-chlorophenyl)-6,7-dimethoxy-1,2,3,4-tetrahydroisoquinoline **6** (Chart 1) by a conventional multistep synthetic approach starting from 6,7-dimethoxyphenethyl alcohol (**7**) and 4-chlorobenzaldehyde (**8**) (Scheme 1, Method A).<sup>7</sup> Considering that the advent of microwave irradiation allows medicinal chemists to rapidly optimize reaction conditions for the preparation of active molecules, we now report a new efficient high-speed microwave-assisted synthesis of racemate **6** optimizing the chemical yield and purity as well as greatly reducing the reaction times (Scheme 1, Method B), analogously to that reported for similar molecules.<sup>12</sup> In particular, we prepared the imine **9** in solvent-free conditions, which in the same reactor was transformed into (*R,S*)-(4'-chlorophenyl)-6,7-dimethoxy-1,2,3,4-tetrahydroisoquinoline (**10**) (Scheme 1, Method A) and then into (*R,S*)-2-acetyl-1-(4'-chlorophenyl)-6,7-dimethoxy-1,2,3,4-tetrahydroisoquinoline (**6**) (Scheme 1, Method B).

oxyphenethyl alcohol (**7**) and 4-chlorobenzaldehyde (**8**) (Scheme 1, Method A).<sup>7</sup> Considering that the advent of microwave irradiation allows medicinal chemists to rapidly optimize reaction conditions for the preparation of active molecules, we now report a new efficient high-speed microwave-assisted synthesis of racemate **6** optimizing the chemical yield and purity as well as greatly reducing the reaction times (Scheme 1, Method B), analogously to that reported for similar molecules.<sup>12</sup> In particular, we prepared the imine **9** in solvent-free conditions, which in the same reactor was transformed into (*R,S*)-(4'-chlorophenyl)-6,7-dimethoxy-1,2,3,4-tetrahydroisoquinoline (**10**) (Scheme 1, Method A) and then into (*R,S*)-2-acetyl-1-(4'-chlorophenyl)-6,7-dimethoxy-1,2,3,4-tetrahydroisoquinoline (**6**) (Scheme 1, Method B).



**Scheme 1.** Reagents and conditions: Method A i—dry toluene, reflux, 180 min; ii—TFA, reflux, 90 min; iii—Ac<sub>2</sub>O, reflux, 90 min. Method B i—P/W 280 W, 90 °C, 5 min; ii—TFA, P/W 280 W, 90 °C, 5 min; iii—Ac<sub>2</sub>O, 7 °C, 3 min.

droisoquinoline (**10**) in the presence of TFA in good yield; then **10** was acetylated to give racemate **6**. It was resolved by chiral HPLC which enabled us to directly, rapidly, and efficiently obtain both enantiomers in high optical purity in a single step. A preliminary analytical study was performed to determine the stationary and mobile phases that allowed the best enantiomeric separations (see [Supplementary data](#)) and afterwards, the semi-preparative chromatographic process was used to collect the two eluted fractions. A chiral stationary phase was employed, that is, Chiralcel® OD consisting of derivatized cellulose; *n*-hexane was used as the mobile phase, with the addition of different percentages of isopropyl alcohol as the organic modifier ([Fig. 1](#)). The best enantioseparations were generally obtained with the lowest alcohol content. With low temperature the separation of enantiomers was better than at high temperature, as shown in [Figure 2a](#) and [b](#). The collected fractions from each isomer were pooled and evaporated under vacuum to give residues, that were recrystallized from diethyl ether to furnish the two enantiomers named **6a** and **6b**.

Their anticonvulsant effects were evaluated against audiogenic seizures in DBA/2 mice. The anticonvulsant efficacies of enantiomers **6a** and **6b** were compared with those of (*R,S*)-2-acetyl-1-(4'-chlorophenyl)-6,7-dimethoxy-1,2,3,4-tetrahydroisoquinoline (**6**). As reported in [Table 1](#) compounds **6**, **6a**, and **6b** protect DBA/2 mice in audiogenic test after intraperitoneal (ip) administration but at different levels of potency. The  $ED_{50} = 4.10 \mu\text{mol/kg}$  (clonic phase) value of compound **6b** suggests that the anticonvulsant effects of (*R,S*)-2-acetyl-1-(4'-chlorophenyl)-6,7-dimethoxy-1,2,3,4-tetrahydroisoquinoline (**6**) reside mainly in the most active (*R*)-enantiomer **6b**, whose absolute configuration has been confirmed by X-ray crystallographic data ([Table 2](#) and [Supplementary data](#)).

We also investigated the effects of compounds **6**, **6a**, and **6b** on membrane currents evoked by AMPA in single rat olfactory cortical brain slice neurons in vitro, under voltage clamp conditions using a fixed dose (0.5  $\mu\text{M}$ ). [Figure 3](#) clearly shows that **6b** is more potent

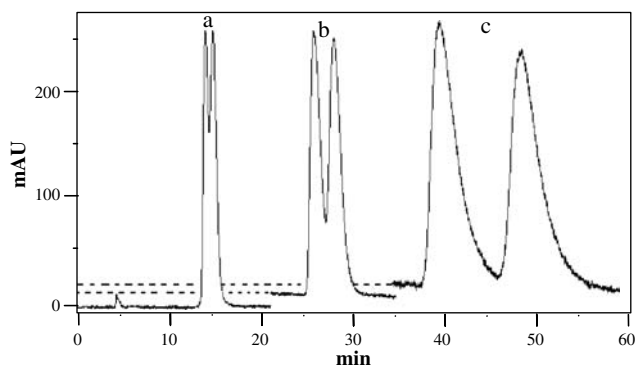


**Figure 1.** Chromatograms of compound **6** on Chiralcel® OD column. Mobile phase: (a) *n*-hexane–isopropyl alcohol, 80:20 (v/v); (b) *n*-hexane–isopropyl alcohol, 90:10 (v/v); (c) *n*-hexane–isopropyl alcohol, 95:5 (v/v);  $T = 20^\circ\text{C}$ ;  $F = 1.0 \text{ mL min}^{-1}$ . UV detection at 284 nm.

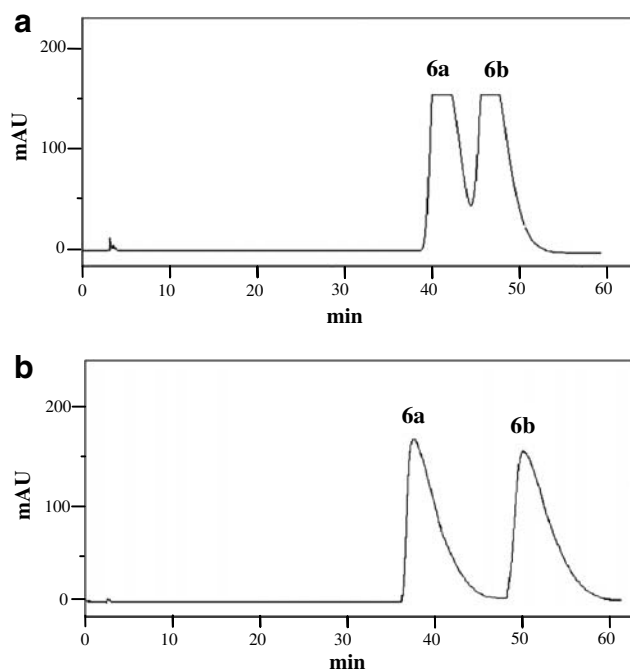


**Figure 2.** Chromatograms of compound **6** on semi-preparative Chiralcel® OD column, mobile phase: *n*-hexane–isopropyl alcohol, 95:5 (v/v),  $F = 5.0 \text{ mL min}^{-1}$ ; (a)  $T = 25^\circ\text{C}$ ; (b)  $T = 15^\circ\text{C}$ .

**Table 1.** Anticonvulsant activity of tetrahydroisoquinolines (**6**, **6a**, and **6b**) against audiogenic seizures in DBA/2 mice

Compound	$ED_{50}$ ( $\mu\text{mol/kg}^a$ )	
	Clonus	Tonus
<b>6</b>	6.51 (4.92–8.61)	3.53 (2.62–4.52)
<b>6a</b> ( <i>S</i> )	22.4 (16.6–32.8)	11.2 (9.03–13.8)
<b>6b</b> ( <i>R</i> )	4.10 (2.53–6.65)	2.05 (1.41–2.98)

<sup>a</sup> All data were calculated according to the method of Litchfield and Wilcoxon. At least 32 animals were used to calculate each  $ED_{50}$ .  $\pm 95\%$  confidence limits are given in parentheses.

than both **6a** and **6**, thus confirming the results obtained in vivo against audiogenic seizures in DBA/2 mice ([Table 1](#)). The clear depression of the apparent maximum of the AMPA dose–response relation demonstrated that both enantiomers **6a** and **6b** act via a non-competitive blockade of the AMPA receptor/ion channel complex.

The crystal structure of **6b**, the more potent of the two enantiomers, was determined by X-ray diffractometry. The ORTEP representation in [Figure 4](#) shows the molecular structure and the atom numbering scheme. The tetrahydroisoquinoline skeleton is present as the core of **6b**. As shown in prior structural studies,<sup>13</sup> the methoxy groups on the benzene-fused ring tend to lie on the aromatic mean plane, therefore a quite large fragment of this molecule is planar. However the substituents to the  $\text{sp}^3$  hybridized carbon atoms diverge from the mentioned planar moiety, as expected. The molecule shows one chiral carbon atom C1 ([Fig. 4](#)) and, since the space group ( $P2_1$ ) found is chiral, and just one molecule is present in the asymmetric unit, the solid state is

**Table 2.** Crystal data and structure refinement of compound **6b**

Empirical formula	C <sub>19</sub> H <sub>20</sub> ClNO <sub>3</sub>
Formula weight	345.81
Temperature	293(2) K
Wavelength	0.71073 Å
Crystal system	Monoclinic
Space group	P2(1)
<i>Unit cell dimensions</i>	
<i>a</i> = 9.0570(2) Å, $\alpha$ = 90°	
<i>b</i> = 9.7800(2) Å, $\beta$ = 107.7010(6)°	
<i>c</i> = 10.6480(2) Å, $\gamma$ = 90°	
Volume	898.52(3) Å <sup>3</sup>
<i>Z</i>	2
Density (calculated)	1.278 mg/m <sup>3</sup>
Absorption coefficient	0.228 mm <sup>-1</sup>
<i>F</i> (000)	364
Crystal size	0.3 × 0.24 × 0.12 mm <sup>3</sup>
$\theta$ range for data collection	2.01 to 28.22°
Index ranges	−12 ≤ <i>h</i> ≤ 12, −8 ≤ <i>k</i> ≤ 12, −14 ≤ <i>l</i> ≤ 14
Reflections collected	16,971
Independent reflections	3825 [ <i>R</i> (int) = 0.0200]
Completeness to $\theta$ = 0.50°	0.0%
Absorption correction	None
Refinement method	Full-matrix least-squares on <i>F</i> <sup>2</sup>
Data/restraints/parameters	3825/7/219
Goodness-of-fit on <i>F</i> <sup>2</sup>	1.055
Final <i>R</i> indices [ <i>I</i> > 2σ( <i>I</i> )]	<i>R</i> <sub>1</sub> = 0.0312, <i>wR</i> <sub>2</sub> = 0.0803
<i>R</i> indices (all data)	<i>R</i> <sub>1</sub> = 0.0362, <i>wR</i> <sub>2</sub> = 0.0840
Absolute structure parameter	0.11(6)
Extinction coefficient	0.014(3)
Largest diff. peak and hole	0.144 and −0.184 e Å <sup>-3</sup>

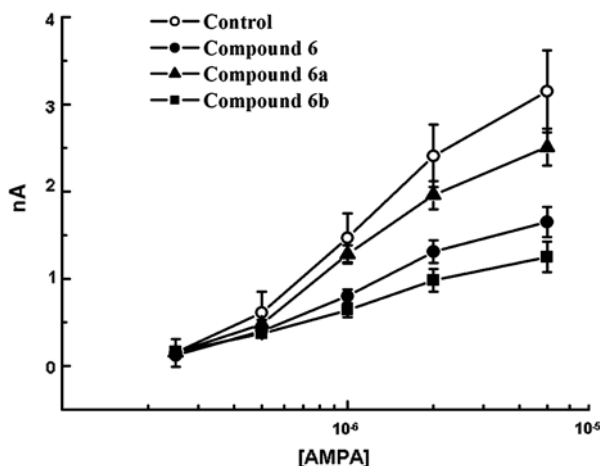


**Figure 3.** Non-competitive type depression of AMPA dose–response relation in the presence of 1,2,3,4-tetrahydroisoquinoline derivatives **6**, **6a** and **6b**. Peak inward membrane currents induced by AMPA were measured in rat olfactory cortical brain slice neurons voltage clamped at −70 mV in the presence of 1 μM TTX. Points represent pooled means (± SEM; nA) plotted against applied AMPA concentration (0.25–5 M, log scale) in the absence (○; *N* = 7) and presence of 0.5 μM compound **6** (●; *N* = 5), **6a** (▲; *N* = 7) or **6b** (■; *N* = 8).

constituted by one enantiomer. The final resolution assessed that the configuration at C1 is *R*, according to the Flack<sup>14</sup> parameter = 0.11(6) found. Crystal packing is mainly maintained by non-conventional hydrogen

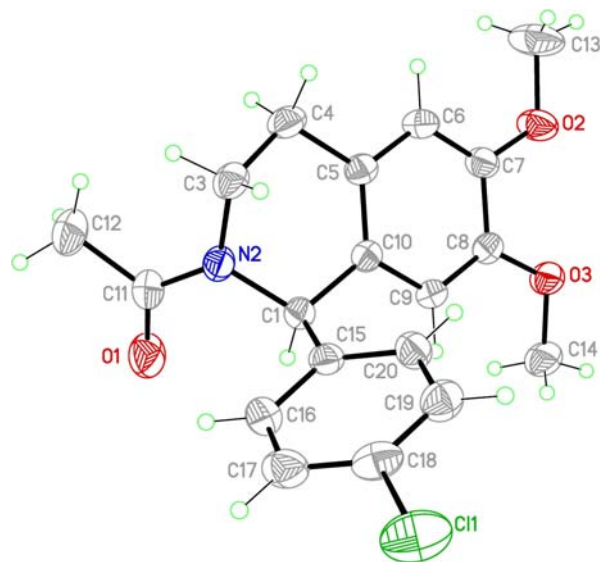


**Figure 4.** ORTEP representation of the (*R*)-enantiomer (**6b**).

bond interactions involving aromatic C–H as donors, and O1 and O2 as acceptors.

Using the results obtained we thought it would be interesting to perform molecular modeling studies in order to further verify the validity of our recently developed 3D predictive pharmacophore model for 1-aryl-6,7-dimethoxy-1,2,3,4-tetrahydroisoquinolines.<sup>15</sup> The best statistical hypothesis, generated by HypoGen module of Catalyst 4.9, consisted of five features: two hydrogen bond acceptors (HBA1–HBA2), two hydrophobic features (HY1–HY2), one hydrophobic aromatic region (HYAr), and three excluded volumes (E1–E3), with a correlation coefficient of 0.919 (see Supplementary data). Figure 5 represents the alignment of the two enantiomers **6a** and **6b** into this pharmacophore model. It is interesting to note that the only (*R*)-enantiomer (**6b**) (Fig. 5a) maps well onto the five chemical functionalities of the 3D pharmacophore model. In particular, the two hydrogen bond regions were occupied by the carbonyl oxygen of the acetyl moiety and the oxygen atom of methoxy group at C-6, the aryl group filled the aromatic hydrophobic feature, whereas the 7-methoxy group and 4'-substituent overlapped with the two hydrophobic sites. In contrast, the (*S*)-enantiomer (**6a**), characterized by lower potency, was able to map only four of the five features thus lacking the suitable conformation for the interaction with the hydrophobic site HY1 (Fig. 5b). In fact, the 7-methoxy substituent is not able to occupy this sphere, corroborating that this molecule could be less active and indicating a specific interaction of the enantiomer in the binding pocket. The HypoGen model also accurately estimated the anticonvulsant potency of **6a** and **6b**. Compound **6b** was predicted to be the most active enantiomer estimating an ED<sub>50</sub> value of 4.18 μmol/kg, comparable to the experimental one (Table 1), whereas for compound **6a**, the HypoGen model estimated an ED<sub>50</sub> value of 41 μmol/kg.



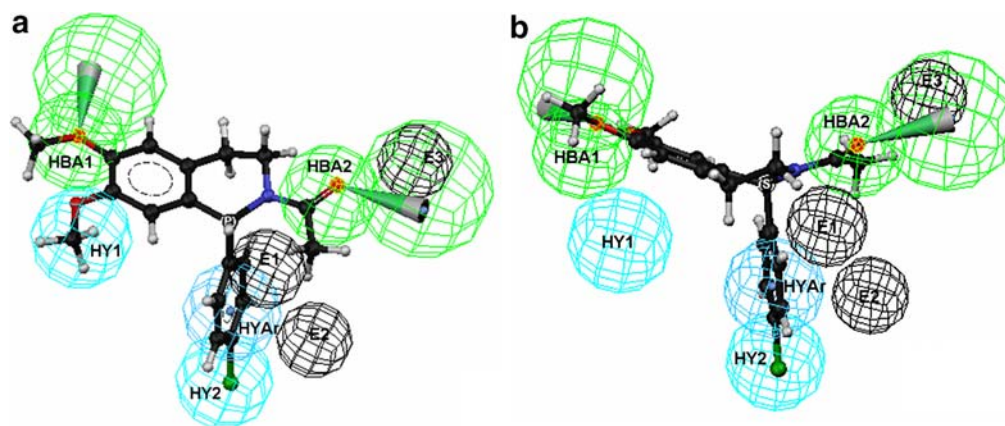


**Figure 5.** Best HypoGen pharmacophore model aligned to compounds **6b** (a) and **6a** (b). The pharmacophore features are color-coded as follows: green, hydrogen bond acceptors (HBA1 and HBA2); blue, hydrophobic aromatic region (HYAr); cyan, hydrophobic groups (HY1 and HY2); black, excluded volumes (E1, E2; E3).

### 3. Conclusion

In conclusion, we herein report a high-speed solvent-free synthetic approach and a direct and rapid resolution, by chiral HPLC, of (*R,S*)-2-acetyl-1-(4'-chlorophenyl)-6,7-dimethoxy-1,2,3,4-tetrahydroisoquinoline (**6**). In addition the absolute stereochemistry of the *R*-enantiomer has been assigned based on X-ray diffractometric data. Finally molecular modeling studies allowed us to explain the higher AMPA antagonistic and anticonvulsant effects of the *R*-enantiomer **6b** thus suggesting that the stereochemical properties influence the pharmacobiological profile of this class of highly potent non-competitive AMPAR antagonists containing the tetrahydroisoquinoline skeleton.

### 4. Experimental

#### 4.1. Chemistry

Microwave-assisted reactions were carried out in a CEM focused Microwave Synthesis System. Melting points were determined on a Stuart SMP10 apparatus and are uncorrected. Elemental analyses (C, H, N) were carried out on a Carlo Erba Model 1106 Elemental Analyzer and the results are within  $\pm 0.4\%$  of the theoretical values. Merck silica gel 60 F<sub>254</sub> plates were used for analytical TLC. <sup>1</sup>H NMR spectra were measured in CDCl<sub>3</sub> with a Varian Gemini 300 spectrometer; chemical shifts are expressed in  $\delta$  (ppm) relative to TMS as internal standard and coupling constants (*J*) in Hz.

**4.1.1. Synthesis of (*R,S*)-1-Aryl-6,7-dimethoxy-1,2,3,4-tetrahydroisoquinoline (**6**).** A mixture of 2-(3',4'-dimethoxyphenyl)ethylamine (**7**) (1.0 mmol) and 4-chlorobenzaldehyde **8** (1.2 mmol) was placed in a cylindrical quartz tube ( $\varnothing$ 2 cm), then stirred and irradiated in a microwave oven at 280 W for 5 min at 90 °C; after cooling to room temperature trifluoroacetic acid (2 mL) was added to crude product **9** obtained in the previous step and the mixture was irradiated at 280 W for 5 min at 90 °C. The reaction was quenched by adding water, and the

mixture was basified (pH  $\approx$ 8–9) with sodium hydroxide to give the isoquinoline derivative as a solid. The crude product was collected by filtration and purified by crystallization with EtOH to afford compound **10**. A solution of 1-(4'-chlorophenyl)-6,7-dimethoxy-1,2,3,4-tetrahydroisoquinoline (**10**) (1 mmol) in Ac<sub>2</sub>O (1 mL) was irradiated in a microwave oven at 280 W for 3 min at 70 °C; after cooling the reaction was quenched by adding water, and the organic layer was extracted with CHCl<sub>3</sub>. The organic layer was dried over Na<sub>2</sub>SO<sub>4</sub>, and the solvent was removed until dryness under reduced pressure. The oil residue was washed with Et<sub>2</sub>O, and the crude product was crystallized with EtOH to give compound **6**. Spectral data for compounds **6**, **9**, and **10** are in line with the literature.<sup>7</sup>

#### 4.2. Chiral liquid chromatography

HPLC grade *n*-hexane and isopropyl alcohol were used, from Merck (Germany). The solutions were filtered prior to injection through Sartorius Minisart®-SRP 15 PTFE 0.45  $\mu$ m filters (Germany), using a 1 mL glass syringe (Poulten & Graf GmbH, Germany). A Shimadzu® LC-10 AD *VP* solvent delivery module was employed for the analyses, connected to a SPD-M10A *VP* UV/Vis photodiode array detector and controlled by EZ-START v7.2 SP1 Chromatography Software by Shimadzu®. A Rheodyne® 8125 injector with a 200  $\mu$ L loop was used for semi-preparative analyses. The semi-preparative column was: Chiralcel® OD 10  $\mu$ m, 25 cm  $\times$  1 cm id stainless steel, packed with cellulose tris-(4-methyl-phenylbenzoate) ester and cellulose tris-(3,5-dimethyl-phenylcarbamate) absorbed on microporous silica gel (Chiralcel® OD Daicel Chemical Industries, J.T. Baker, The Netherlands). The column was thermostated with a Merck Hitachi L-7003 column oven. Solutions of the compounds (0.5 mg mL<sup>-1</sup>) in isopropyl alcohol were filtered through the 0.45  $\mu$ m membrane, stored at 4 °C, and replaced weekly. Three eluents were used: *n*-hexane–isopropyl alcohol, 80:20, v/v (eluent A); *n*-hexane–isopropyl alcohol, 90:10, v/v (eluent B); *n*-hexane–isopropyl alcohol, 95:5, v/v (eluent C). Flow rate was kept at 1.0 mL min<sup>-1</sup> throughout the

study, and the column temperature was set at 20 °C. Detection was done at 284 nm. The influence of operating temperature on the enantioresolution was afterwards investigated using eluant A in the 15–35 °C range (steps of 5 °C). HPLC conditions for separation in the semi-preparative column were: *n*-hexane–isopropyl alcohol, 95:5, v/v, flow rate was kept at 5.0 mL min<sup>-1</sup>, and the column temperature was set at 15 °C.

### 4.3. Pharmacology

**4.3.1. Testing of anticonvulsant activity.** All experiments were performed with DBA/2 mice that are genetically susceptible to sound-induced seizures.<sup>7</sup> DBA/2 mice (8–12 g; 22–25 days old) were purchased from Harlan Italy (Corezzano, Italy). Groups of 10 mice of either sex were exposed to auditory stimulation for 30 min following administration of vehicle or each dose of drugs studied.

**4.3.2. Statistical analysis.** Statistical comparisons between groups of control and drug-treated animals were made using Fisher's exact probability test (incidence of the seizure phases). The ED<sub>50</sub> values of each phase of audiogenic seizures were determined for each dose of compound administered, and dose–response curves were fitted using a computer program by Litchfield and Wilcoxon's method.

**4.3.3. Electrophysiology.** Transverse slices of olfactory cortex were obtained from 150–200 g male Wistar rats as previously described<sup>16</sup> and stored in oxygenated Krebs solution before being transferred to an immersion chamber for recordings. The following compounds were tested: AMPA, **6**, **6a**, and **6b**. In addition, slices were continuously superfused with 1 μM TTX, to block voltage-activated sodium currents, and induced repetitive firing at the peak of AMPA responses. AMPA and TTX were freshly prepared in Krebs solution, whereas compounds **6**, **6a**, and **6b** were pre-dissolved in DMSO to give 1 mM stock solutions, and subsequently diluted in Krebs solution (containing 0.1–1% v/v DMSO), immediately prior to use. These concentrations of DMSO had no deleterious effects on neuronal membrane properties or AMPA-induced inward currents. All measurements were performed before, during, and after bath application of pharmacological agents so that each neuron served as its own control.

### 4.4. X-ray crystal structure determination

A single crystal of compound **6b** (for crystal data, see [Supplementary data](#)) suitable for X-ray single-crystal analysis was obtained at room temperature by slow evaporation from Et<sub>2</sub>O. The intensities were collected at 298 K on a Bruker APEX 8 diffractometer with graphite-monochromated Mo Kα radiation (λ = 0.71073 Å). The data collection, cell refinement, and reduction were carried out with the SMART and SAINT programs.<sup>17</sup> Software used for structure solution, refinement, analysis, and drawing include SIR2004, SHELXL97, PARST95, XP all handled by the WINGX package.<sup>18</sup>

The structure of compound **6b** has been deposited in the Cambridge Crystallographic Data Centre, reference number CCDC 633704.

### 4.5. Molecular modeling

Compounds **6a** and **6b** were sketched within Catalyst and minimized to their closest local energy minimum using a molecular mechanics approach. Poled conformations were generated for each molecule using the 'Best' conformer generation option and an energy cutoff of 10 kcal/mol. Pharmacophore model has been generated with the HypoGen module of Catalyst 4.9 using a training set of 1,2,3,4-tetrahydroisoquinoline derivatives.<sup>15</sup>

### Acknowledgment

Financial support for this research by Università of Messina and MIUR is gratefully acknowledged.

### Supplementary data

Supplementary data for HPLC study, evaluation of anticonvulsant properties, electrophysiological study, HypoGen pharmacophore model, and X-ray crystallographic data associated with this article can be found in the online version, at [doi:10.1016/j.bmc.2007.05.059](https://doi.org/10.1016/j.bmc.2007.05.059).

### References and notes

1. Kew, J. N.; Kemp, J. A. *Psychopharmacology (Berl)* **2005**, 179, 4.
2. Gressens, P.; Spedding, M.; Gigler, G.; Kertesz, S.; Villa, P.; Medja, F.; Williamson, T.; Kapus, G.; Levay, G.; Szenasi, G.; Barkoczy, J.; Harsing, L. G., Jr. *Eur. J. Pharmacol.* **2005**, 519, 58.
3. De Sarro, G.; Gitto, R.; Russo, E.; Ibbadu, G. F.; Barreca, M. L.; De Luca, L.; Chimirri, A. *Curr. Top. Med. Chem.* **2005**, 5, 31.
4. Weiser, T. *Curr. Drug Targets CNS Neurol. Disord.* **2005**, 4, 153.
5. Catarzi, D.; Colotta, V.; Varano, F. *Med. Res. Rev.* **2007**, 27, 239.
6. Barreca, M. L.; Gitto, R.; Quartarone, S.; De Luca, L.; De Sarro, G.; Chimirri, A. *J. Chem. Inf. Comput. Sci.* **2003**, 43, 651.
7. Gitto, R.; Barreca, M. L.; De Luca, L.; De Sarro, G.; Ferreri, G.; Quartarone, S.; Russo, E.; Constanti, A.; Chimirri, A. *J. Med. Chem.* **2003**, 46, 197.
8. Gitto, R.; Caruso, R.; Pagano, B.; De Luca, L.; Citraro, R.; Russo, E.; De Sarro, G.; Chimirri, A. *J. Med. Chem.* **2006**, 49, 5618.
9. Ferreri, G.; Chimirri, A.; Russo, E.; Gitto, R.; Gareri, P.; De Sarro, A.; De Sarro, G. *Pharmacol. Biochem. Behav.* **2004**, 77, 85.
10. Rizzo, M.; Ventrice, D.; De Sarro, G.; Gitto, R.; Caruso, R.; Chimirri, A. *J. Chromatogr. B Analyt. Technol. Biomed. Life Sci.* **2005**, 821, 15.
11. Arstad, E.; Gitto, R.; Chimirri, A.; Caruso, R.; Constanti, A.; Turton, D.; Hume, S. P.; Ahmad, R.; Pilowsky, L. S.; Luthra, S. K. *Bioorg. Med. Chem.* **2006**, 14, 4712.

12. Pal, B.; Jaisankar, P.; Giri, V. S. *Synth. Commun.* **2003**, *33*, 2339.
13. Bruno, G.; Nicolo, F.; Rotondo, A.; Gitto, R.; Zappala, M. *Acta Crystallogr. C* **2001**, *57*, 1225.
14. Flack, H. D. *Acta Crystallogr. A* **1983**, *39*, 876.
15. De Luca, L.; Gitto, R.; Barreca, M. L.; Caruso, R.; Quartarone, S.; Citraro, R.; De Sarro, G.; Chimirri, A. *Arch. Pharm. (Weinheim)* **2006**, *339*, 388.
16. Constanti, A.; Bagetta, G.; Libri, V. *Neuroscience* **1993**, *56*, 887.
17. SMART V. 5.060 and SAINT V. 6.02 Softwares. Bruker AXS Inc.: Madison, W., 1999.
18. Farrugia, L. J. *J. Appl. Crystallogr.* **1999**, *32*, 837.